SF2A 2013
L. Cambrésy, F. Martins, E. Nuss and A. Palacios (eds)

TOWARDS 3D SIMULATIONS OF CEPHEIDS STARS

S. Félix[1], E. Audit[1] and B. Dintrans[2]

Abstract. We are using the HERACLES hydrodynamic simulation code, to construct simplified 1D and 2D simulations of the kappa-mechanism following Gastine's results obtained with the PENCIL CODE. In this proceeding, we focus on the conduction step for stable and unstable setups, in 1D and 2D with convection. We thus show that we are reproducing PENCIL CODE's results quite well.

Keywords: Cepheid, kappa-mechanism, convection, pulsations, nonlinear simulations, HERACLES

1 Introduction

Cepheids are giant stars displaying periodic variations of luminosity and radius. This phenomenon was explained by Eddington (1917) through the κ-mechanism, an excitation mechanism of stellar oscillations that is related to sharp changes of opacity in ionisation regions.

A simplified κ-mechanism model (the propagation of radial acoustic waves in a partially ionised shell in 1D and 2D cartesian boxes) has been previously investigated with the PENCIL CODE by Gastine & Dintrans (in particular, refer to Gastine & Dintrans (2008), hereafter GD2008). We intend to extend this work to 3D simulations with the hydrodynamic code HERACLES from CEA, France. First step is getting hydrodynamic equilibria and was presented in SF2A 2012 proceedings (Félix et al. (2012)).

Hydrodynamics and gravity equations are solved with an explicit scheme (second order in time & space) on a cartesian-fixed grid of physical size $l \times L$, with constant spacing Δx. In this proceeding, we will focus on the implicit conduction step of HERACLES.

2 Conduction step

In the conduction step, we are solving $c_v\,\rho\,\frac{\partial T}{\partial t} - \vec{\nabla}\cdot(\kappa\vec{\nabla}T) = 0$ where κ denotes the conductivity, T the temperature, ρ the density and c_v the heat capacity at constant volume. Temperatures are normalized to the surface temperature.

The κ-mechanism implies that opacity sharply increases in a definite region of the star envelope. In our code, this opacity bump is shaped by a radiative conductivity hollow, since opacity and conductivity are inversely proportional. The hollow is parametrized as follows:

- $T_{\rm bump}$ is its position in the temperature profile and 3 cases are investigated: $T_{\rm bump} = [1.7,\ 2.1,\ 2.8]$;
- σ is its slope, with $\sigma = 7$ as a standard value;
- $2 * e$ is its FWHM and we usually take $e = 0.4$.

Following GD2008, conductivities κ only depend on temperature and are calculated using the following formula:

$$\kappa(T) = \kappa_{\rm max}\left[1 + \mathcal{A}\frac{-\Pi/2 + \arctan(\sigma T^{+}T^{-})}{\Pi/2 + \arctan(\sigma e^2)}\right],$$

[1] Maison de la Simulation, CEA/CNRS/INRA/U-PSUD/UVSQ (USR 3441), 91191 Gif-sur-Yvette, France
[2] IRAP, CNRS/Université de Toulouse (UMR5277), 14 av. Edouard Belin, F-31400 Toulouse, France

where

$T^{\pm} = T - T_{\rm bump} \pm e$;

$\mathcal{A} = \dfrac{\kappa_{\rm max} - \kappa_{\rm min}}{\kappa_{\rm max}}$, the relative amplitude of the conductivity extrema $\kappa_{\rm max}$ and $\kappa_{\rm min}$;

and $T_{\rm bump}$, σ and e are the already-defined hollow parameters.

2.1 Numerical scheme

HERACLES uses a finite-volume Godunov method. The timestep dt is therefore limited by stability conditions imposing that $\mathrm{dt} \leqslant \min(\mathrm{dt}_{\rm hydro}, \mathrm{dt}_{\rm gravity}, \mathrm{dt}_{\rm radiative\ diffusion}) \leqslant \mathrm{dt}_{\rm radiative\ diffusion}$. Typical dt in that case are $\mathrm{dt} \simeq 10^{-6}$. It leads to lengthy wall times and an implicit scheme has been implemented for the conduction step. As a consequence, the dynamics of the simulation becomes only constrained by the speed of sound and typical dt are now $\mathrm{dt} \simeq 10^{-3}$. This implicit scheme can be used at the first or second order and a simple input parameter allows to switch between both accuracies. Finally, in our simulations, opacities may be given either in an explicit or implicit form.

2.2 Growth rates

The hydrodynamic equilibrium with conduction is perturbed on velocity by the eigenfunctions of the unstable fundamental mode. These eigenfunctions were calculated by GD2008 for our three cases $T_{\rm bump} = [1.7,\ 2.1,\ 2.8]$ and are shown in Figure 1.

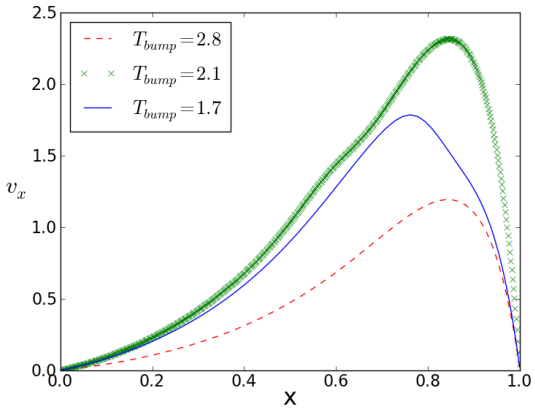

Fig. 1: Eigenfunctions of the unstable fundamental mode (real part of velocity) for $T_{\rm bump} = 1.7$ (solid line), $T_{\rm bump} = 2.1$ (crossed line) and $T_{\rm bump} = 2.8$ (dashed line). Calculations were made by GD2008.

$T_{\rm bump}$	n_x	τ
1.7	512	-2.63×10^{-2}
2.1	512	$+1.97 \times 10^{-2}$
2.8	512	-2.14×10^{-2}

Table 1: Growth rates τ of the mean vertical momentum $< \rho u_x >$ for different setups: $T_{\rm bump}$ is the position of the hollow in the temperature profile and n_x is the number of points along the gravity-directed x-axis of our simulation box.

We then studied the temporal evolution of the mean vertical momentum $< \rho u_x >$ (averaged over the box) and calculated its growth rate τ during the linear phase ($t \lesssim 50$). Results are summarized in Table 1, while Figure 2 shows the corresponding evolutions with time.

Only one setup (hollow with $T_{bump} = 2.1$, green line on Figure 2) is unstable with a positive growth rate. This corresponds to the instability conditions in which the κ-mechanism is efficient, given by GD2008:

1. the hollow has a sufficient slope: $\dfrac{d\kappa_{\rm T}}{dx} < 0$ where $\kappa_{\rm T} = \dfrac{\partial \ln \kappa}{\partial \ln T}$.
2. the instability zone is well located: $\psi = \dfrac{< c_v T_{\rm transition} > \Delta m}{PL} \approx 1$, with P the acoustic mode period and L the luminosity.

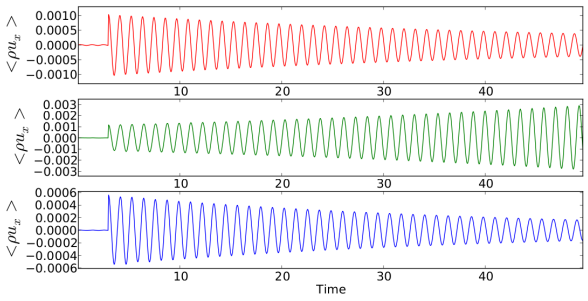

Fig. 2: Temporal evolution of the mean vertical momentum $< \rho u_x >$ for $T_{\rm bump} = 2.8$ (**Upper panel**), $T_{\rm bump} = 2.1$ (**Middle panel**) and $T_{\rm bump} = 1.7$ (**Lower panel**). The perturbation in velocity is added at $t = 3$.

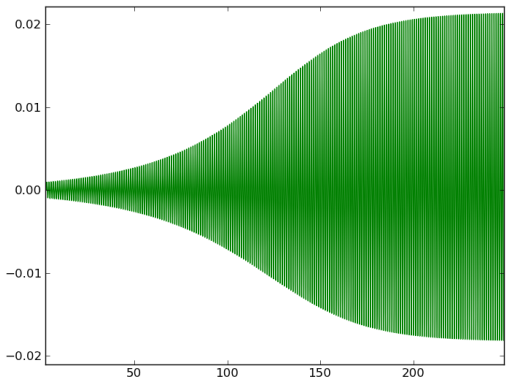

Fig. 3: Temporal evolution of the mean vertical momentum $< \rho u_x >$ for $T_{\rm bump} = 2.1$.

With these criteria, the other two setups ($T_{\rm bump} = 1.7$ and $T_{\rm bump} = 2.8$) are stable because the instability zone is respectively too close or too far from the surface to maintain instability. This shows on Table 1 since $\tau < 0$ for both cases.

One oscillation takes approximatively 1.15 units of time (43 oscillations in a bit less than 50 units of time), which corresponds quite well to what GD2008 got with the PENCIL CODE.

2.3 Nonlinear saturation

Unstable simulations with the initial setup $T_{\rm bump} = 2.1$ keep a positive growth rate until they reach their nonlinear limit-cycle stability, where the mean vertical momentum oscillates between two definite values (see the final plateau at late times in Figure 3). It occurs around $t \approx 200$, which agrees well with the characteristic timescale of instability given by $1/\tau \approx 100$. The dynamics and values of this saturation are also compatible with GD2008's results.

3 Cepheids in 2D

Now that hydrodynamic, gravity and conduction steps are available and accurate, we can go further on to 2D simulations. We choose new setups known to trigger convection (Gastine & Dintrans (2011), hereafter GD2011). As we aim at studying convection-pulsation coupling, conductivity profiles are now shaped such that the temperature gradient becomes superadiabatic around the conductivity hollow and convection may develop there (the so-called Schwarzschild's criterion).

We focused on profiles named G6 and G8 in GD2011 that proved to be the more relevant ones. Figure 4 is similar to Figure 3 in GD2008 but for both G6 and G8 simulations. It shows the conductivity (with the hollow), temperature, density and $d\kappa_{\rm T}/dx$ profiles for these two setups. On the latest, we see that these simulations are set in order to fulfill the first instability condition around the hollow. Convection is indeed triggered as we do observe convection plumes in Figure 6.

Temporal evolution of the mean vertical momentum $< \rho u_x >$ for these two setups (Figure 5) shows that the G6 one is stable while the G8 one is unstable, as GD2011 predicted.

Please note that high resolution simulations are mandatory to properly represent the instability. Numerically speaking, to save computational time and cost, we are doing this conduction step once every ten steps without altering the behaviours or results.

4 Conclusions

With HERACLES, we managed to reproduce GD2008's results (obtained with PENCIL CODE) quite well concerning 1D hydrodynamical simulations with conduction. These simulations show oscillations of the mean vertical

momentum $< \rho u_x >$, leading to a nonlinear saturation for the unstable setup. 2D simulations trigger convection and show a stable or unstable behaviour depending on the initial setup, accordingly to GD2008's and GD2011's results. Finally, we started long-awaited 3D simulations of this convection-pulsations interaction and will present our results in a forthcoming paper.

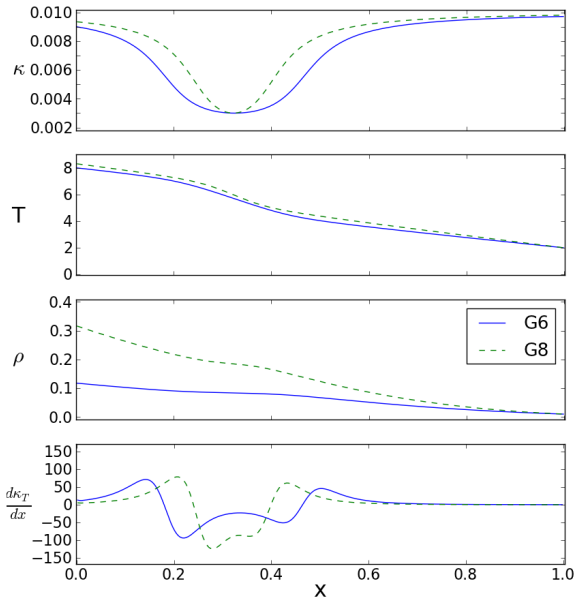

Fig. 4: Conductivity (**Upper panel**), temperature (**Second panel**), density (**Third panel**) and $\frac{d\kappa_T}{dx}$ (**Lower panel**) profiles for G6 and G8 simulations.

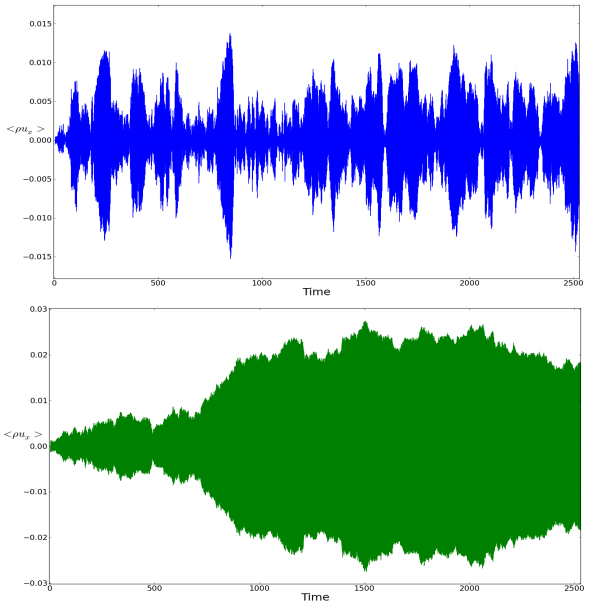

Fig. 5: Temporal evolution of the mean vertical momentum $< \rho u_x >$ for setups G6 (**Upper panel**) and G8 (**Lower panel**).

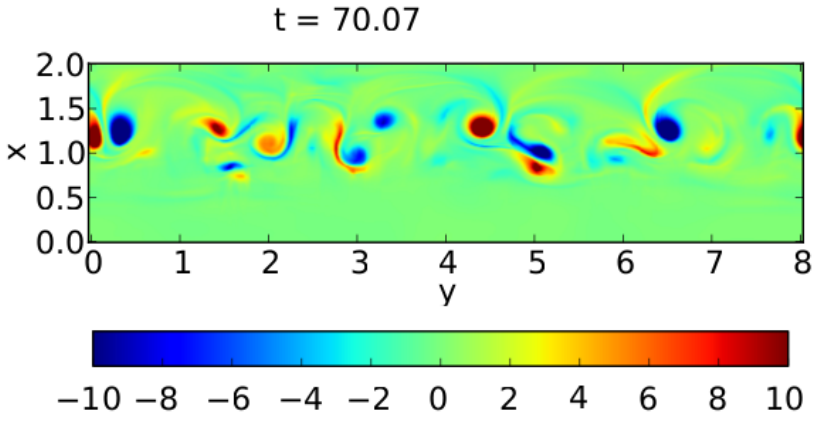

Fig. 6: Snapshot of the vorticity field $\vec{\nabla} \times \vec{u}$ in the 2D model G6 with convection and κ-mechanism.

References

Eddington, A. S. 1917, The Observatory, 40, 290

Félix, S., Audit, E., & Dintrans, B. 2012, in SF2A-2012: Proceedings of the Annual meeting of the French Society of Astronomy and Astrophysics, ed. S. Boissier, P. de Laverny, N. Nardetto, R. Samadi, D. Valls-Gabaud, & H. Wozniak, 329–332

Gastine, T. & Dintrans, B. 2008, A&A, 484, 29

Gastine, T. & Dintrans, B. 2011, A&A, 528, A6